BIOCHEMICAL PHARMACOLOGY 72 (2006) 838–849

available at www.sciencedirect.com

ScienceDirect

journal homepage: www.elsevier.com/locate/biochempharm

Kinetics of nonpeptide antagonist binding to the human gonadotropin-releasing hormone receptor: Implications for structure–activity relationships and insurmountable antagonism

Susan K. Sullivan [a,1], Sam R.J. Hoare [b,1,*], Beth A. Fleck [a], Yun-Fei Zhu [c], Christopher E. Heise [a], R. Scott Struthers [d], Paul D. Crowe [a]

[a] Department of Pharmacology and Lead Discovery, Neurocrine Biosciences Inc., 12790 El Camino Real, San Diego, CA 92130, United States
[b] Department of Discovery Biology, Neurocrine Biosciences Inc., 12790 El Camino Real, San Diego, CA 92130, United States
[c] Department of Medicinal Chemistry, Neurocrine Biosciences Inc., 12790 El Camino Real, San Diego, CA 92130, United States
[d] Department of Endocrinology, Neurocrine Biosciences Inc., 12790 El Camino Real, San Diego, CA 92130, United States

ARTICLE INFO

Article history:
Received 2 June 2006
Accepted 17 July 2006

Keywords:
Gonadotropin-releasing hormone
G-protein-coupled receptor
Dissociation rate constant
Receptor kinetics
Nonpeptide antagonist
Structure–activity relationship

ABSTRACT

Numerous nonpeptide ligands have been developed for the human gonadotropin-releasing hormone (GnRH) receptor as potential agents for treatment of disorders of the reproductive-endocrine axis. While the equilibrium binding of these ligands has been studied in detail, little is known of the kinetics of their receptor interaction. In this study we evaluated the kinetic structure–activity relationships (SAR) of uracil-series antagonists by measuring their association and dissociation rate constants. These constants were measured directly using a novel radioligand, [^{3}H] NBI 42902, and indirectly for unlabeled ligands. Receptor association and dissociation of [^{3}H] NBI 42902 was monophasic, with an association rate constant of $93 \pm 10\ \mu M^{-1}\ min^{-1}$ and a dissociation rate constant of $0.16 \pm 0.02\ h^{-1}$ ($t_{1/2}$ of 4.3 h). Four unlabeled compounds were tested with varying substituents at the 2-position of the benzyl group at position 1 of the uracil (–F, $–SO(CH_3)$, $–SO_2(CH_3)$ and $–CF_3$). The nature of the substituent did not appreciably affect the association rate constant but varied the dissociation rate constant >50-fold ($t_{1/2}$ ranging from 52 min for $–SO(CH_3)$ to >43 h for $–CF_3$). This SAR was poorly resolved in standard competition assays due to lack of equilibration. The functional consequences of the varying dissociation rate were investigated by measuring antagonism of GnRH-stimulated [^{3}H] inositol phosphates accumulation. Slowly dissociating ligands displayed insurmountable antagonism (decrease of the GnRH E_{max}) while antagonism by more rapidly dissociating ligands was surmountable (without effect on the GnRH E_{max}). Therefore, evaluating the receptor binding kinetics of nonpeptide antagonists revealed SAR, not evident in standard competition assays, that defined at least in part the mode of functional antagonism by the ligands. These findings are of importance for the future definition of nonpeptide ligand SAR and for the identification of potentially useful slowly dissociating antagonists for the GnRH receptor.

* *Corresponding author*. Tel.: +1 858 617 7678; fax: +1 858 617 7601.
E-mail address: shoare@neurocrine.com (Sam R.J. Hoare).

[1] The authors contributed equally.

0006-2952/$ – see front matter
doi:10.1016/j.bcp.2006.07.011

1. Introduction

Gonadotropin-releasing hormone (GnRH) is a linear decapeptide secreted from the hypothalamus into the portal circulation. GnRH binds to the GnRH receptor on gonadotroph cells in the anterior pituitary. GnRH receptor activation stimulates the synthesis and release of luteinizing hormone (LH) and follicle stimulating hormone (FSH), which bind to gonadal receptors, stimulating the synthesis of the sex steroid hormones estrogen and testosterone [1]. The GnRH receptor is a seven transmembrane domain G-protein coupled receptor (GPCR) belonging to the class A family of GPCRs. [2]. The GnRH receptor signals predominantly through the GTP binding proteins $G\alpha_q$ and $G\alpha_{11}$, stimulating phosphatidyl inositol turnover by phospholipase C, mobilization of intracellular calcium, diacylglycerol formation, protein kinase C activation, and arachidonic acid release [3].

GnRH peptide agonists have been used therapeutically to modulate the reproductive endocrine axis in a variety of disorders including precocious puberty, endometriosis, prostate cancer, uterine fibroids, breast cancer, and fertility disorders [4,5]. Overall, gonadal suppression is observed with GnRH agonist peptide therapy, an effect that results from desensitization and down regulation of pituitary GnRH receptors [5]. Although GnRH agonist peptides have proven to be clinically effective, there are several drawbacks to this approach, including initial stimulation of the pituitary and subsequent increases in LH, FSH, and sex steroids prior to the GnRH receptor down regulation. The hormonal ''flare'' seen with GnRH agonist peptides can be avoided by the use of GnRH peptide antagonists, such as abarelix and cetrorelix, which bind pituitary GnRH receptors without stimulating FSH and LH release [6–8]. However, treatment with agonist and antagonist peptides requires parenteral administration and typically involves depot formulation. Consequently, considerable effort has been directed towards development of orally active non-peptide GnRH receptor antagonists [9,10].

Many novel small molecules have been synthesized to understand the structure activity relationships of antagonist binding affinities for the GnRH receptor [11–16] (reviewed in Refs. [9,10]). However, little is known about the binding kinetics of these ligands to the GnRH receptor. Evaluation of receptor binding kinetics can provide an additional dimension for the understanding of ligand pharmacology [17–20]. For example, measuring receptor–ligand binding kinetics of slowly equilibrating ligands can reveal structure–activity relationships (SAR) that can be masked or distorted in measurements of apparent equilibrium binding affinity, owing to lack of equilibration of ligand with receptor in competition assays [18,20–23]. Slow antagonist dissociation from receptors can affect the mode of functional antagonism. *In vitro*, this effect can reduce the maximal response of an agonist in functional antagonism experiments ('insurmountable antagonism') [17,24–31]. *In vivo*, slow receptor-antagonist dissociation has been proposed to prolong and enhance antagonist efficacy, for example candesartan blockade of the angiotensin type 1 (AT_1) receptor in rats [26] and humans [32,33]. Here, we evaluated the kinetic SAR of a series of nonpeptide antagonists for the GnRH receptor, employing a novel nonpeptide radioligand, [^{3}H] NBI 42902. This SAR was then used to investigate the relationship between the kinetics of ligand binding and the mode of functional antagonism of GnRH-stimulated cellular signaling.

2. Materials and methods

2.1. Materials

All chemicals and reagents were purchased from either Sigma–Aldrich (St. Louis, MO) or Fisher Scientific (Los Angeles, CA) unless otherwise stated. Synthesis of NBI 42902 (Fig. 1), (1-(2,6-difluorobenzyl)-3-[(2R)-amino-2-phenethyl]-5-(2-fluoro-3-methoxyphenyl)-6-methyluracil, has been described previously [12]. Synthesis of three other uracil antagonists (Fig. 1) was performed using modifications to the method described [12]: Uracil-1, 1-(2-fluoro, 6-methanesulfonylbenzyl)-3-[(2R)-amino-2-phenethyl]-5-(2-fluoro-3-methoxyphenyl)-6-methyluracil); Uracil-2, (1-(2-flouro,6-methanesulfinylbenzyl)-3-[(2R)-amino-2-phenethyl]-5-(2-fluoro-3-methoxyphenyl)-6-methyluracil); Uracil-3 (1-(2-flouro,6-trifluoromethylbenzyl)-3-[(2R)-amino-2-phenethyl]-5-(2-fluoro-3-methoxyphenyl)-6-methyluracil). Compounds were stored at 6 mM concentration in dimethylsulfoxide at −20 °C. [^{3}H] NBI 42902 (Fig. 1) was prepared by American Radiolabeled Chemical Inc. (St. Louis, MO). Briefly, NBI 42902 was treated with boron tribromide, followed by di *t*-butyl dicarbonate to yield the corresponding boc-protected phenol which was then treated with tritium-labeled iodomethane in the presence of potassium carbonate in dimethylformamide, followed by de-protection of the boc group with trifluoroacetic acid to yield the desired product, which was purified by HPLC to greater than 99% purity. The final material had a specific activity of 80 Ci/mmol and was stored in ethanol at −20 °C. Fetal bovine serum (FBS) was purchased from Hyclone Laboratories (Logan, UT), dialyzed FBS was from Gibco (Carlsbad, CA), Geneticin (G418 sulfate) was from Cellgro (Herndon, VA), and inositol-free media was obtained from Specialty Media (Phillipsburg, NJ). Myo-2-[^{3}H] inositol was purchased from Amersham Biosciences (Newark, NJ). UniFilter 350 and UniFilter GF/C plates were from Whatman (Clifton, NJ), 96 well low binding plates were obtained from Corning (Palo Alto, CA), and Lumaplates were purchased from PerkinElmer Life Sciences (Boston, MA). AG1-X8 Dowex Resin was obtained from BioRad (Hercules, CA).

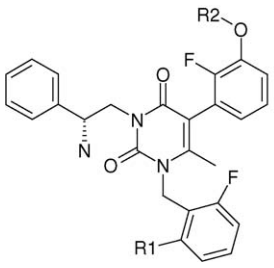

Ligand	R1	R2
[^{3}H] NBI 42902	F	$C(^3H)_3$
NBI 42902	F	CH_3
Uracil 1	$SO(CH_3)$	CH_3
Uracil 2	$SO_2(CH_3)$	CH_3
Uracil 3	CF_3	CH_3

Fig. 1 – Chemical structure of [^{3}H] NBI 42902, NBI 42902, and closely related uracil nonpeptide antagonists for the human GnRH receptor.

2.2. Expression of the human GnRH receptor and preparation of cell membranes

Expression of the GnRH receptor has been described elsewhere [13,34]. Briefly, the cDNA of the human receptor was cloned into pcDNA3.1 (+) mammalian expression vector (Invitrogen, Carlsbad, CA). Rat basophilic leukemia cells (RBL-1 cells, ATCC, Manassas, VA) were stably transfected using lipofectamine (Invitrogen, Carlsbad, CA), and a high expressing single cell clone was isolated and maintained in Dulbecco's Modified Eagles Medium (DMEM), supplemented with 10% FBS, 10 mM HEPES, 2 mM L-glutamine, 1 mM sodium pyruvate, 0.1 mM non-essential amino acids, 50 IU/ml penicillin, 50 μg/ml streptomycin, and 250 μg/ml Geneticin. RBL cells were used in this study because they provided the highest level of GnRH receptor expression (compared with, for example, transfected HEK293 cells). For isolation of cell membranes, these cells were harvested using 0.5 mM EDTA in phosphate-buffered saline then collected by centrifugation at 800 × *g* for 10 min at 4 °C. The cell pellet was resuspended in tissue buffer at 4 °C (1.5 mM KH_2PO_4, 8.1 mM Na_2HPO_4, 2.7 mM KCl, and 138 mM NaCl, 10 mM $MgCl_2$, 2 mM EGTA, pH 7.4) and transferred to a pressure cell. N_2 was applied to the cell at a pressure of 900 psi for 30 min at 4 °C, and cells were lysed by release of the pressure. Unbroken cells and larger debris were removed by centrifugation at 1200 × *g* for 10 min at 4 °C. The remaining cell membrane fraction was centrifuged at 45,000 × *g* for 20 min at 4 °C and the resulting membrane pellet resuspended in assay buffer (see below). Total protein in the isolated cell membrane fraction was determined with the Coomassie Plus Protein Reagent kit (Pierce, Rockford, IL) using bovine serum albumin as the standard. Membrane aliquots were stored at −80 °C until use.

2.3. Radioligand binding assays

Radioligand saturation binding experiments were performed by the addition of cell membranes to low protein-binding 96 well plates containing various concentrations of [^{3}H] NBI 42902 ranging from approximately 50 pM to 5 nM in assay buffer (50 mM Tris, 150 mM NaCl, 5 mM $MgCl_2$, and 0.5 mM EDTA, pH 7.5). Duplicate determinations of total binding and nonspecific binding (defined using 10 μM NBI 42902) were performed. The assay mixture (total volume of 200 μl) was incubated for 2 h at room temperature and terminated by rapid vacuum filtration onto Unifilter GF/C filter plates. GF/C filter plates were pretreated with 0.5% polyethylenimine in distilled water for 30 min. Filters were pre-rinsed with 200 μl per well assay buffer using a cell harvester (UniFilter-96 Filtermate; Packard, PerkinElmer Life Sciences). After filtration, membranes were washed two times with 250 μl ice-cold buffer (0.01% Tween-20, in phosphate buffered saline, pH 7.4). Filter plates were dried, 50 μl scintillation fluid added (Microscint 20; PerkinElmer Life Sciences), and the plate monitored for radioactivity using a TopCount NXT at 30% efficiency(PerkinElmer Life Sciences). The total amount of radioligand added to the assay was measured using a 1600TR liquid scintillation counter (PerkinElmer Life Sciences) at 47% efficiency.

Radioligand association experiments were initiated by the addition of cell membranes to wells containing various concentrations of [^{3}H] NBI 42902 ranging from approximately 100 pM to 2 nM (final concentration) in assay buffer (total assay volume of 200 μl). Duplicate determinations of total binding and nonspecific binding (defined using 10 μM NBI 42902) were performed. Following incubation at room temperature for varying times, bound radioligand was harvested as described above. Specific binding for each concentration of radioligand was determined by subtracting nonspecific binding from total binding. The association experiments conducted to determine the receptor kinetic rate constants of the unlabeled ligands were performed in the same manner as the association experiments described above, using a single concentration of [^{3}H] NBI 42902 (approximately 1 nM). Association was measured in the absence of unlabeled ligand and in the presence of a range of five concentrations of unlabeled ligand. Radioligand dissociation experiments were performed by pre-incubating cell membranes with 1 nM [^{3}H] NBI 42902 for 1 h. Dissociation was initiated by the addition of 10 μM NBI 42902 (final concentration). Bound radioligand was harvested at the indicated time points using the method described above. Non-specific binding was measured by including 10 μM NBI 42902 in the pre-incubation phase of the experiment. In each experiment, one duplicate set of wells did not receive 10 μM NBI 42902 in the dissociation phase of the experiment, in order to measure the stability of total [^{3}H] NBI 42902 binding over time. Total binding remained stable for at least 6 h (data not shown).

[^{3}H] NBI 42902 displacement experiments were performed by the addition of cell membranes to low protein-binding 96 well plates containing various concentrations of unlabeled ligand (ranging from 32pM to 10 μM) and [^{3}H] NBI 42902 (approximately 1 nM final concentration), in a total volume of 200 μl. Following incubation at room temperature for 2 h, bound radioligand was harvested as described above.

2.4. Measurement of inositol phosphates accumulation

The procedure used was a modified version of published protocols [35]. RBL-1 cells expressing the GnRH receptor were seeded into 96 well plates at a density of 15,000 cells per well in inositol-free DMEM containing 10% dialyzed FBS, 10 mM HEPES, 2 mM L-glutamine, 1 mM sodium pyruvate, 0.1 mM non-essential amino acids, 50 IU/ml penicillin and 50 μg/ml streptomycin, and labeled for 48 h with 0.2 μCi per well myo-2-[^{3}H] inositol. The cells were washed once in buffer containing 140 mM NaCl, 4 mM KCl, 20 mM HEPES, 8.3 mM glucose, 1 mM $MgCl_2$, 1 mM $CaCl_2$, 10 mM LiCl, and 0.1% BSA. Buffer alone or non-peptide antagonist in this buffer was applied to the cells (six concentrations within the range of 1 nM–3 μM), then 30 s later native GnRH peptide was added at concentrations ranging from 30 pM to 10 μM. Cells were incubated for 1 h at 37 °C under a humidified atmosphere of 5% CO_2. Cells were then extracted with 10 mM formic acid at 4 °C for 30 min and the lysate was applied to 20 μg Dowex AG1-X8 resin loaded into UniFilter 350 96-well plates. The resin was washed once in H_2O, once in 60 mM ammonium formate/5 mM sodium tetraborate, and inositol phosphates were eluted with 1 M ammonium formate/0.1 M formic acid. The eluate was transferred to a Lumaplate, dried at 37 °C, and radioactivity counted in a TopCount NXT.

2.5. Data and statistical analysis

All data were analyzed using Prism 4.0 (GraphPad Software, La Jolla, CA). Radioligand saturation data were analyzed using a method that accounts for ligand depletion, as previously described [36]. Data were fit to one- and two-site saturation equations and the best fit determined using a partial *F*-test. A single site binding model fit best for all saturation binding experiments ($p > 0.05$).

Association binding data (specific binding) were fit to monophasic and biphasic association equations and the best fit determined using a partial *F*-test. A monophasic model fit best for all experiments ($p > 0.05$), as follows:

$$Y = Y_{t\to\infty}(1 - e^{-k_{obs}t}) \quad (1)$$

where t is time in min, k_{obs} the observed association rate constant, Y the specific binding at time t and $Y_{t\to\infty}$ is specific binding at infinite t. To determine the association rate constant (k_{+1}) of [^{3}H] NBI 42902, k_{obs} was plotted against the [^{3}H] NBI 42902 concentration, and the data analyzed by linear regression. The slope of this fit is equivalent to the association rate constant. The r^2 for these fits was >0.94 for all experiments. Dissociation binding data (specific binding) were fit to monophasic and biphasic dissociation equations, with the plateau of the specific binding set to zero, and the best fit determined using a partial *F*-test. A monophasic model fit best ($p > 0.05$), as follows:

$$Y = Y_{t=0}\, e^{-k_{-1}t} \quad (2)$$

where k_{-1} is the dissociation rate constant, t time in min, Y specific binding at time t, and $Y_{t=0}$ is specific binding at the initiation of the dissociation phase of the assay.

The association and dissociation rate constants of unlabeled ligands were measured using the method of Motulsky and Mahan [18], in which association of a labeled radioligand is measured in the absence and presence of the unlabeled test ligand. The analysis assumes the model in Scheme 1.where R is receptor, L the radioligand, k_{+1} the radioligand association rate constant, k_{-1} the radioligand dissociation rate constant, I the unlabeled ligand, k_{+2} the unlabled ligand association rate constant, and k_{-2} is the unlabled ligand dissociation rate constant. Kinetic constants for the unlabeled ligand were determined by measuring the time course of association of [^{3}H] NBI 42902 in the absence of unlabeled ligand and in the presence of multiple concentrations of unlabeled ligand. Specific binding data (RL) were fit globally to the following equation [18]:

$$\mathrm{RL} \underset{k_{-1}}{\overset{k_{+1}}{\rightleftharpoons}} \mathrm{R} + \mathrm{L} + \mathrm{I} \underset{k_{-2}}{\overset{k_{+2}}{\rightleftharpoons}} \mathrm{RI}$$

Scheme 1

$$[\mathrm{RL}] = \frac{B_{max}k_1[\mathrm{L}]}{K_F - K_S} \times \left[\frac{k_{-2}(K_F - K_S)}{K_F K_S} + \frac{K_{-2} - K_F}{K_F}\, e^{-K_F t} - \frac{k_{-2} - K_S}{K_S}\, e^{-K_S t}\right] \quad (3)$$

where

$$K_A = k_{+1}[\mathrm{L}] + k_{-1}, \qquad K_B = k_{+2}[\mathrm{I}] + k_{-2},$$
$$K_F = 0.5(K_A + K_B + \sqrt{(K_A - K_B)^2 + 4k_{+1}k_{+2}[\mathrm{L}][\mathrm{I}]}),$$
$$K_S = 0.5(K_A + K_B - \sqrt{(K_A - K_B)^2 + 4k_{+1}k_{+2}[\mathrm{L}][\mathrm{I}]}).$$

The fitted parameters were B_{max}, k_{+1}, k_{+2}, and k_{-2}. The fixed parameters were k_{-1}, [L] and [I]. The association rate constant of [^{3}H] NBI 42902 (k_{+1}) was fit for each experiment as an internal control. k_{+1} determined by the global fit was not statistically different from the k_{+1} determined by direct measurement of [^{3}H] NBI 42902 association alone (Table 1) for any of the experiments run (data not shown). One limitation of this analysis, discovered by data simulation and experience with the fitting, is that the dissociation rate constant for the unlabeled ligand (k_{-2}) cannot be accurately determined if this

Table 1 – Association and dissociation rate constants of [^{3}H] NBI 42902 and unlabeled nonpeptide antagonists for the GnRH receptor

Ligand	R1-group	Association rate constant		Dissociation rate constant	
		k_{+1} or k_{+2} (M^{-1} min^{-1})	k_{+1} or k_{+2} $t_{1/2}$ at 1 nM (min)	k_{-1} or k_{-2} (h^{-1})	k_{-1} or k_{-2} $t_{1/2}$ (h)
[^{3}H] NBI 42902	F	93 ± 10	7.2	0.16 ± 0.02	4.3
NBI 42902	F	23 ± 3	27	0.20 ± 0.02	3.5
Uracil-1	$SO(CH_3)$	8.4 ± 1.1	31	0.80 ± 0.17	0.87
Uracil-2	$SO_2(CH_3)$	21 ± 5	32	0.050 ± 0.009	14
Uracil-3	CF_3	30 ± 5	23	≤0.016	>43

Association and dissociation rate constants of [^{3}H] NBI 42902 (k_{+1} and k_{-1}) were determined directly (see Fig. 2B–D), whereas the association and dissociation rate constants of the unlabeled ligands (k_{+2} and k_{-2}) were determined indirectly using Eq. (3) as described in Section 2.5 (see Fig. 3) Ligand structures are shown in Fig. 1. Data for the rate constants are mean ± S.E.M. from three to four experiments, except NBI 42902 ($n = 12$). $t_{1/2}$ values were calculated from the mean rate constant, using Eqs. (4) and (5). For Uracil-3 only an upper limit of the dissociation rate constant could be determined; data simulations using Eq. (3) indicated that k_{-2} could only be determined accurately if the value is more than 0.1 times the value of k_{-1}. Rate constants for unlabeled ligands were compared using single-factor ANOVA, followed by the Newman–Keuls post-test comparing the value for each ligand. This analysis demonstrated significant difference between the association rate constants ($p < 0.05$) with the only significant difference indicated in the post-test between Uracil-1 and Uracil-3 ($p < 0.05$). The dissociation rate constants were significantly different ($p < 0.001$) with the post-test indicating NBI 42902, Uracil-1 and Uracil-2 were significantly different from each other ($p < 0.05$). Uracil-3 was excluded from the dissociation rate constant analysis because the absolute value could not be determined.

value is <0.1 times the dissociation rate constant of the radioligand (k_{-1}).

The rate constant values were used to determine the half-life ($t_{1/2}$) of ligand association at 1 nM (Eq. (4)), and ligand dissociation (Eq. (5)):

$$\text{association } t_{1/2} \text{ at } 1\,\text{nM} = \frac{0.693}{10^{-9}k_{+2} + k_{-2}} \quad (4)$$

$$\text{dissociation } t_{1/2} = \frac{0.693}{k_{-2}} \quad (5)$$

Measured and simulated [^{3}H] NBI 42902 displacement by unlabeled ligands was fit to a single-affinity state competition equation. For inositol phosphates accumulation assays, data were analyzed using a sigmoidal dose-response equation with slope factor fixed at unity (the slope was fixed at unity for both displacement and inositol phosphates accumulation assays because initial analyses using a four parameter-logistic equation indicated a slope close to unity, typically 0.9–1.1). The logarithm of the concentration of antagonist was plotted against the log of the dose ratio minus one, and analyzed by linear regression to obtain the x-intercept (logarithm of the concentration of antagonist required to double the GnRH EC_{50}, formally $-pA_2$ for antagonists that do not decrease the GnRH E_{max} – NBI 42902 and Uracil-1).

3. Results

3.1. GnRH receptor binding of [^{3}H] NBI 42902

In order to assess the kinetics of nonpeptide ligand interaction with the GnRH receptor we developed a novel radioligand, [^{3}H] NBI 42902 (Fig. 1) and characterized its interaction with the receptor. [^{3}H] NBI 42902 (1 nM concentration) bound membranes from RBL cells expressing the human GnRH receptor with a total binding:nonspecific binding ratio of typically 3:1, with no specific binding detected in membranes from non-transfected RBL cells. Saturation binding of [^{3}H] NBI 42902 indicated the radioligand bound with high affinity ($pK_d = 9.70 \pm 0.04$, $K_d = 200$ pM, $n = 5$) to a

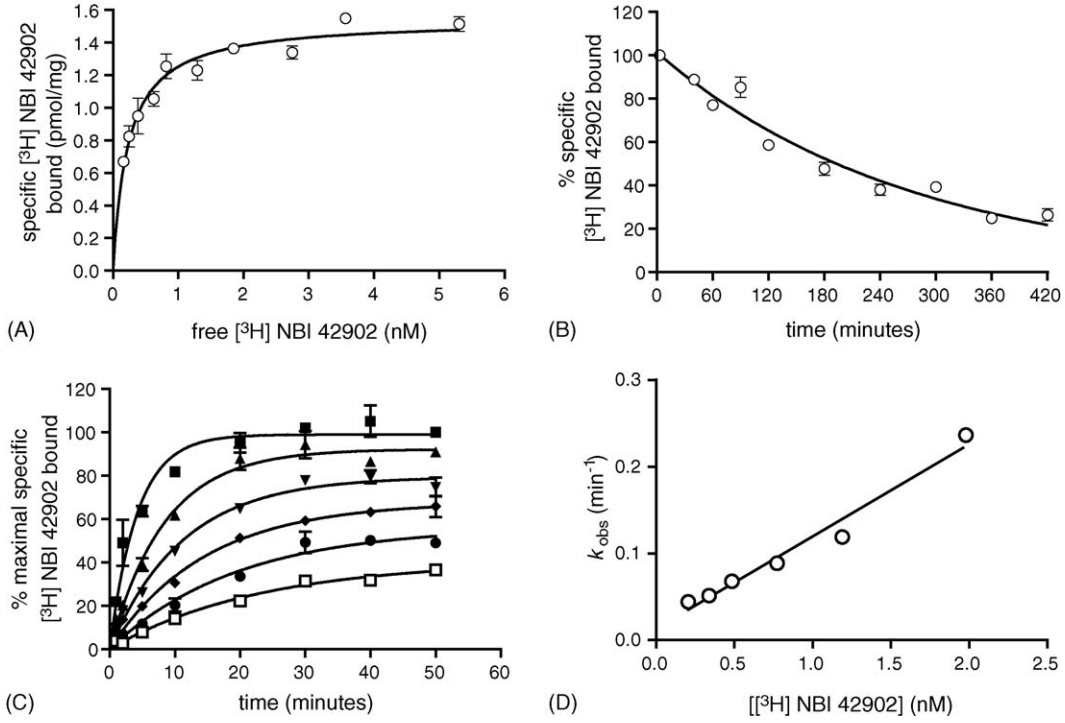

Fig. 2 – GnRH receptor binding of [^{3}H] NBI 42902. (A) Saturation binding to membranes from RBL cells stably expressing the human GnRH receptor. The radioligand concentration given on the x-axis is the free concentration, calculated by subtracting total binding from the total radioligand added. K_d and B_{max} values were determined by fitting the data to a single affinity state saturation equation. Data points are the mean ± S.E.M. of duplicate determinations, and the data are representative of four independent experiments. (B) Dissociation of [^{3}H] NBI 42902 from the GnRH receptor. The dissociation rate constant (k_{-1}) was determined by fitting the data to a monophasic dissociation equation (Eq. (2)). Data points are the mean ± S.E.M. of duplicate determinations, and the data are representative of three independent experiments. (C) Association of [^{3}H] NBI 42902 with the GnRH receptor (concentrations of [^{3}H] NBI 42902 of 210 pM □, 340 pM ●, 480 pM ◆, 770 pM ▼, 1.2 nM ▲, and 2.0 nM ■). The data were fit to a monophasic association equation (Eq. (1)) to determine the observed association rate constant (k_{obs}). Data are normalized to the asymptotic specific binding for 2.0 nM [^{3}H] NBI 42902. Data points are the mean ± S.E.M. of duplicate determinations, and the data are representative of three independent experiments. (D) Determination of the association rate constant k_{+1}. The k_{obs} value from (C) was plotted against the [^{3}H] NBI 42902 concentration, and the slope (k_{+1}) was determined by linear regression (k_{+1} in this experiment of 110 μM^{-1} min^{-1}).

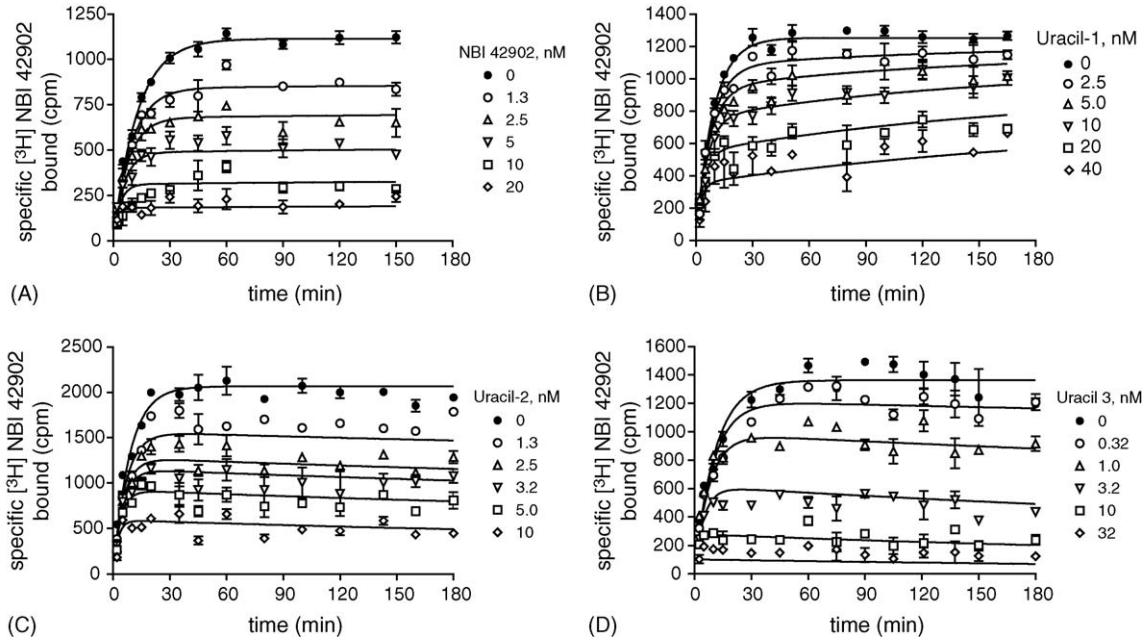

Fig. 3 – Measurement of unlabeled ligand receptor binding kinetics. The association and dissociation rate constants of unlabeled ligands were determined by measuring association of specific binding of [^{3}H] NBI 42902 to membranes from RBL cells expressing the GnRH receptor, alone and in the presence of five concentrations of unlabeled ligand, for NBI 42902 (A), Uracil-1 (B), Uracil-2 (C) and Uracil-3 (D). The curves are the global fits to Eq. (3) (r^2 of 0.96, 0.94, 0.93 and 0.94 for the representative experiments in A, B, C and D, respectively, $r^2 > 0.90$ in all experiments). Nonspecific binding was subtracted from total binding yielding specific binding on the y-axis. Nonspecific binding values for these experiments were: 450, 674, 781 and 450 cpm for A, B, C and D, respectively. Data points are mean ± S.E.M. of duplicate determinations. Data are from representative experiments performed 3–4 times, except NBI 42902 (n = 12).

Table 2 – Nonpeptide antagonist affinity measurements from competition binding, simulated competition binding and kinetic experiments

Ligand	R-group	Competition assay		Kinetic assay	
		Measured pK_i at 2 h (K_i, pM)	Simulated K_i at 2 h (pM)	Simulated equilibrium K_i (pM)	Measured pK_i (K_i, pM)
NBI 42902	–F	10.04 ± 0.09 (90)	120	150	9.82 ± 0.04 (150)
Uracil-1	–SO(CH_3)	9.44 ± 0.17 (360)	700	1600	8.81 ± 0.03 (1500)
Uracil-2	–SO_2(CH_3)	10.19 ± 0.21 (64)	110	41	10.31 ± 0.13 (48)
Uracil-3	–CF_3	10.37 ± 0.26 (44)	71	<9.1	ND

Ligand competition against [^{3}H] NBI 42902 binding to the GnRH receptor in RBL membranes was measured as described in Section 2.3, using an incubation time of 2 h (Fig. 4A). Data were fit to a single affinity-state competition equation and the K_i calculated using the Cheng–Prusoff equation [37], using the kinetically derived K_d for [^{3}H] NBI 42902 (k_{-1}/k_{+1} = 29 pM). pK_i data are the mean ± S.E.M. from three to eight experiments. The simulated K_i from competition assays was determined using simulated [^{3}H] NBI 42902 displacement data. The % displacement of [^{3}H] NBI 42902 binding by unlabeled ligands was calculated using Eq. (3), using the kinetic parameters for [^{3}H] NBI 42902 and unlabeled compound given in Table 1, a [^{3}H] NBI 42902 concentration of 1 nM, and 12 concentrations of unlabeled ligand from 10 μM to 30 pM. These simulated displacement data (Fig. 4B and C) were then fit to a single affinity-state competition equation and the K_i calculated using the Cheng–Prusoff equation [37], using the kinetically derived K_d for [^{3}H] NBI 42902 (k_{-1}/k_{+1} = 29 pM). This simulation was performed for two different incubation times—2 h, representing the simulated K_i in the competition assay; and 430 h, representing the simulated K_i as equilibrium is closely approached (10 times the slowest kinetic parameter measured, the dissociation rate constant $t_{1/2}$ for Uracil-3, Table 1). The ligand dissociation constant measured using the kinetic assay (Fig. 3) was calculated as k_{-2}/k_{+2} (Table 1). For each kinetic experiment the pK_i value was then calculated and the mean ± S.E.M. determined (n = 3–12). Measured pK_i values from competition assays were compared statistically by single-factor ANOVA, which indicated a significant difference between the different ligands ($p < 0.05$). Post-testing with the Newman–Keuls indicated a significant difference between Uracil-1 and the other three compounds ($p < 0.05$), with no significant difference between NBI 42902, Uracil-2 and Uracil-3. The same analysis was applied to the pK_i value measured using the kinetic assay, which indicated the value for NBI 42902, Uracil-1 and Uracil-2 were all significantly different from each other ($p < 0.05$). ND: the kinetic pK_i value for Uracil-3 could not be determined because the absolute value of k_{-2} could not be determined (see legend to Table 1).

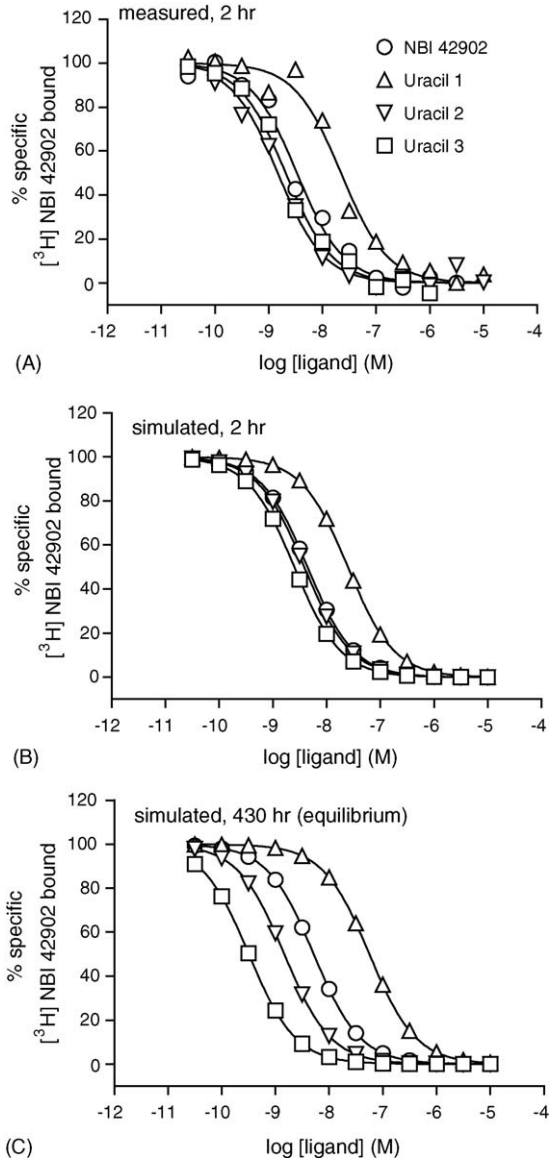

Fig. 4 – Measured and simulated displacement of [^{3}H] NBI 42902 binding by unlabeled nonpeptide antagonists. (A) Measured displacement of [^{3}H] NBI 42902 binding to membranes from RBL cells expressing the GnRH receptor by unlabeled ligands. Data points are single determinations and data are from representative experiments performed three to eight times. (B) Simulated displacement of [^{3}H] NBI 42902 binding by unlabeled ligands at 2 h. The % displacement of [^{3}H] NBI 42902 binding by unlabeled ligands was calculated using Eq. (3), using the kinetic parameters for [^{3}H] NBI 42902 and unlabeled compound (Table 1), a [^{3}H] NBI 42902 concentration of 1 nM, a time interval of 2 h, and 12 concentrations of unlabeled ligand from 10 μM to 30 pM. (C) Simulated displacement of [^{3}H] NBI 42902 binding by unlabeled ligands at 430 h. This time interval represents a close approach to equilibrium for all ligands (10 times the slowest kinetic parameter measured, the dissociation rate constant $t_{1/2}$ for Uracil-3). Note that this time interval (approximately 18 days) is experimentally impractical. In all graphs the curves are fits to a single affinity state competition equation.

single affinity state of the GnRH receptor with a B_{max} of 1.2 ± 0.2 pmol/mg of membrane protein (Fig. 2A). Association of [^{3}H] NBI 42902 with the receptor was monophasic (Fig. 2C), with an association rate constant (k_{+1}) of 93 ± 10 μM^{-1} min^{-1} (Fig. 2D, Table 1). Dissociation of [^{3}H] NBI 42902 from the receptor was also monophasic (Fig. 2B), with a dissociation rate constant (k_{-1}) of 0.16 ± 0.02 h^{-1}, equivalent to a dissociation half-life ($t_{1/2}$) of 4.3 h (Table 1). The kinetically derived K_d (k_{-1}/k_{+1}) for [^{3}H] NBI 42902 was 29 pM. This value is 6.8-fold lower than the K_d value from saturation binding of [^{3}H] NBI 42902. One possible explanation for this difference is that slow dissociation of [^{3}H] NBI 42902 from the receptor ($t_{1/2}$ of 4.3 h) prevents the attainment of equilibrium in the saturation experiments (duration of 2 h) [18]. Equilibrium is closely approached after a time exceeding three-fold the dissociation half-life [18].

3.2. *Association and dissociation rate constants of unlabeled nonpeptide antagonists*

We next aimed to quantify the receptor binding kinetics of unlabeled structural analogues of NBI 42902, to investigate the kinetic SAR of this series of ligands. The method described by Motulsky and Mahan [18] was used to measure the association and dissociation rate constants of the unlabeled ligand (k_{+2} and k_{-2}, respectively, Scheme 1, in Section 2.5). In this method, association of a radioligand with known kinetic parameters is measured in the presence of a fixed concentration of unlabeled ligand and the data analyzed with Eq. (3) (Section 2.5) to yield k_{+2} and k_{-2}. The analysis assumes a competitive interaction between radiolabeled and unlabeled ligands, conditions that were met in this study with the use of closely related unlabeled and radiolabeled nonpeptide antagonists (Fig. 1). We extended this analysis to include multiple concentrations of ligand and a global fit of the data since it provided more reproducible estimates of the kinetic parameters (data not shown). We first tested the validity of this method for the GnRH receptor by comparing the kinetic rate constants of unlabeled NBI 42902 with those for [^{3}H] NBI 42902. Association of [^{3}H] NBI 42902 was measured in the absence of unlabeled ligand and in the presence of five concentrations of NBI 42902 (Fig. 3A). The dissociation rate constant (k_{-2}) for unlabeled NBI 42902 (0.20 ± 0.02 h^{-1}) closely matched that for the radiolabeled ligand (0.16 ± 0.02 h^{-1}, two-tailed *t*-test, $p > 0.05$, Table 1). The association rate constant for unlabeled NBI 42902 (k_{+2} = 23 ± 3 μM^{-1} min^{-1}) was not greatly different (four-fold) from that for [^{3}H] NBI 42902 (k_{+1} = 93 ± 10 μM^{-1} min^{-1}, Table 1). This difference could be explained by slight loss of unlabeled compound upon serial dilution from the 6 mM stock solution to the effective concentrations in the assay (1.3–20 nM), since the effective concentration of unlabeled compound contributes in defining k_{+2} by analysis with Eq. (3).

We then used this method to measure k_{+2} and k_{-2} of close structural analogues of NBI 42902, in which the 2-position substituent of the benzyl group at position 1 of the uracil was varied (R1 is –F for NBI 42902, $-SO(CH_3)$ for Uracil-1, $-SO_2(CH_3)$ for Uracil-2, $-CF_3$ for Uracil-3, Fig. 1). The association rate constant was generally similar for all four ligands, the only significant difference (3.6-fold) being between Uracil-1 and

Uracil-3 (Fig. 3, Table 1). However the dissociation rate constant varied considerably between the ligands. Uracil-1 (–$SO(CH_3)$ at R1) displayed the most rapid dissociation from the receptor ($t_{1/2}$ of 52 min, four-fold faster than NBI 42902 (–F)). Uracil-2 (–$SO_2(CH_3)$) and Uracil-3 (–CF_3) dissociated more slowly than NBI 42902. This effect was graphically manifest as a slight 'overshoot' of [^{3}H] NBI 42902 association in the presence of the unlabeled ligand (initial peak of association declining with time, Fig. 3C and D [18]). For Uracil-2 the dissociation rate was markedly slow ($t_{1/2}$ of 14 h, Fig. 3C, Table 1). For Uracil-3 the dissociation rate was so slow that it could not be determined accurately using this method; analysis using Eq. (3) yielded k_{-2} estimates approaching zero (10^{-7} when k_{-2} was constrained to be >0 in the analysis, see Section 2.5). We found that k_{-2} could not be accurately determined if this value is <0.1 times k_{-1}, the dissociation rate constant of the radioligand (see Section 2.5). For this reason, the upper k_{-2} value limit for Uracil-3 was calculated to be 0.016 h^{-1}, corresponding to a dissociation $t_{1/2}$ of >43 h (Table 1). Taken together, these findings indicate a SAR of the dissociation rate constant at the 2-position substituent of the benzyl group at position 1 of the uracil, with a rank order for $t_{1/2}$ of dissociation of Uracil-3 (–CF_3) > Uracil-2 (–$SO_2(CH_3)$) > NBI 42902 (–F) > Uracil-1 (–$SO(CH_3)$). The difference between the most slowly and rapidly dissociating compounds (Uracil-3 and Uracil-1) was >50-fold (Table 1).

3.3. *Comparison of nonpeptide antagonist affinity measurements from kinetic and standard competition assays*

The analytical method used to measure the kinetics of ligand–receptor interaction was developed in part to determine the affinity of ligands that do not reach equilibrium within the time-frame of standard competition assays [18,20]. Nonpeptide antagonist affinity for the GnRH receptor can be assessed using k_{+2} and k_{-2} from the kinetic structure–activity evaluation above; division of k_{-2} by k_{+2} yields the equilibrium dissociation constant. The dissociation constants for NBI 42902, Uracil-1 and Uracil-3 were significantly different (Table 2, values of 150 pM, 1.5 nM and 48 pM, respectively). Owing to the unmeasurably slow dissociation of Uracil-3 (Table 1), an equilibrium dissociation constant for this ligand could not be determined.

We next aimed to compare ligand affinity determined from kinetic experiments with the apparent affinity (K_i) from a standard competition experiment (competition versus [^{3}H] NBI 42902, Fig. 4A) using a typical 2-h incubation at room temperature. The IC_{50} of the unlabeled ligands was converted to K_i using the Cheng–Prusoff equation [37] using the kinetically derived K_d for [^{3}H] NBI 42902 of 29 pM. Under these conditions the K_i varied only 8.2-fold (Fig. 4A, Table 2). The K_i values for NBI 42902, Uracil-2 and Uracil-3 could not be distinguished statistically (90, 64 and 44 pM, respectively, Table 2). Therefore the SAR that could be well distinguished for these three ligands from kinetic assays (both in terms of k_{-2} (Table 1) and k_{-2}/k_{+2} (Table 2)) was not evident from the competition binding data. Notably the K_i for Uracil-3 was not significantly different from that for NBI 42902, whereas the dissociation rate constant was >10-fold lower.

One likely explanation for the difference between kinetic and competition SAR is a lack of equilibration in the competition binding assay (2 h incubation) owing to slow dissociation of the ligands from the receptor ($t_{1/2}$ > 2 h for NBI 42902, Uracil-2 and Uracil-3) [18]. We tested this hypothesis

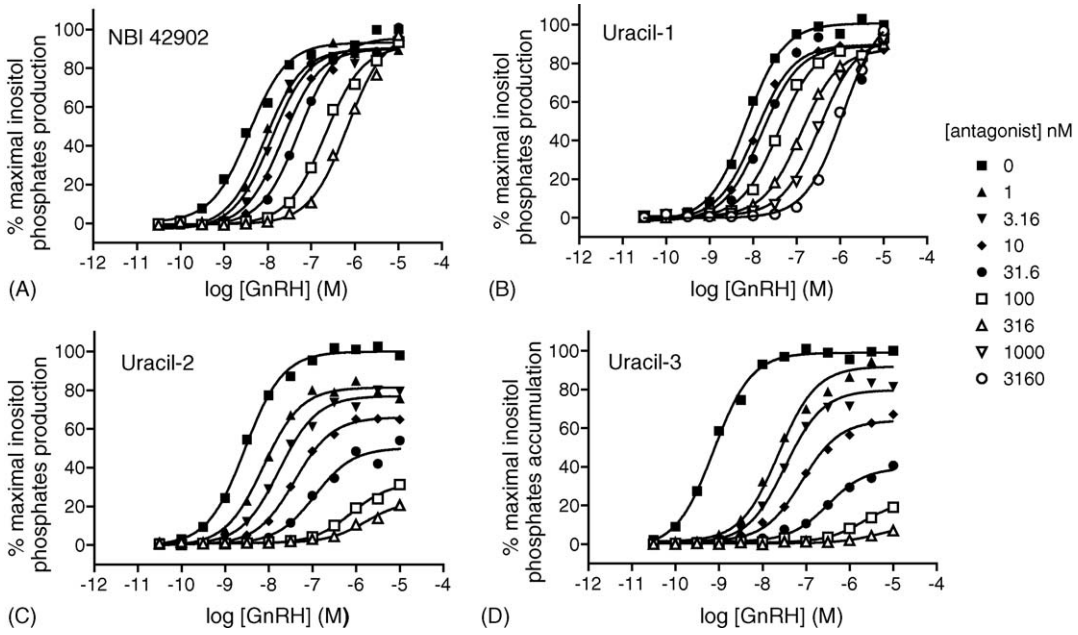

Fig. 5 – Antagonism of GnRH-stimulated inositol phosphates accumulation by nonpeptide antagonists. Inositol phosphates accumulation in RBL cells expressing the human GnRH receptor was measured as described in Section 2. The dose–response to GnRH was determined alone, and in the presence of multiple concentrations of nonpeptide antagonist (A: NBI 42902; B: Uracil-1; C: Uracil-2; D: Uracil-3). Curves are fits to a sigmoid dose–response equation to determine the GnRH EC_{50} and E_{max}. Data points are single determinations. The experiments were performed three or four times with similar results.

quantitatively by simulating the predicted competition binding profile at 2 h. For this simulation Eq. (3) was used to determine predicted inhibition of [^{3}H] NBI 42902 binding by unlabeled ligands (Fig. 4B). The inputs for this simulation were the kinetic parameters for [^{3}H] NBI 42902 and the unlabeled ligands (Table 1), a [^{3}H] NBI 42902 concentration of 1 nM and a time interval of 2 h. The simulated competition data (Fig. 4B) were then fit to a single-state competition equation to determine the IC_{50}, from which the predicted K_i was determined using the k_{-1}/k_{+1} value for [^{3}H] NBI 42902 of 29 pM. In all cases the predicted K_i value closely matched the experimentally determined value (Table 2). This observation provides quantitative verification that the masked SAR in the competition binding experiments arises from lack of equilibration in the competition assay. In order to validate the simulation, a very large time interval was used in the simulation (430 h, 10 times the slowest dissociation $t_{1/2}$) to determine the predicted K_i under conditions in which equilibrium is closely approached [18]. The predicted K_i was then compared with the k_{-2}/k_{+2} value for the unlabeled ligands. In all cases the predicted K_i under equilibrium conditions closely matched the k_{-2}/k_{+2} value measured experimentally (Table 2), validating the simulation.

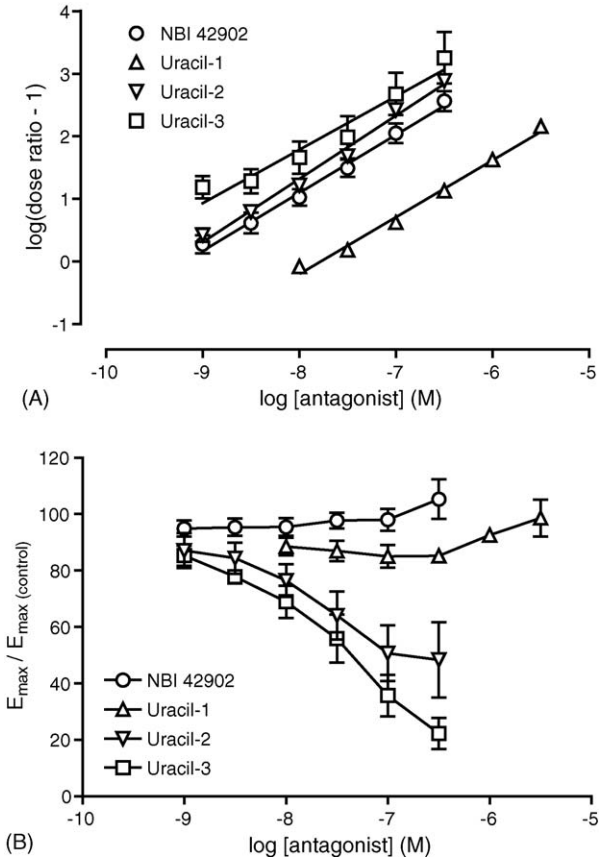

Fig. 6 – Effect of nonpeptide antagonists on the GnRH EC_{50} and E_{max} for stimulation of inositol phosphates accumulation. The GnRH EC_{50} and E_{max} values from experiments represented in Fig. 5 were used to assess the mode of functional antagonism by the ligands. (A) Dose ratio ($EC_{50(+antagonist)}/EC_{50(control)} - 1$). The lines are linear regression fits to the data (slope = 0.90 ± 0.01, 0.90 ± 0.05, 1.01 ± 0.03 and 0.95 ± 0.07 for NBI 42902, Uracil-1, Uracil-2 and Uracil-3, respectively, with corresponding x-axis intercept values of 9.23 ± 0.14, 7.79 ± 0.05, 9.31 ± 0.09 and 9.88 ± 0.22). (B) Effect on E_{max}. Basal inositol phosphates accumulation was subtracted from the maximal accumulation to yield E_{max}. Data points are mean ± S.E.M. from three to four experiments.

3.4. *Functional antagonist profile of nonpeptide antagonists*

Measurements of dissociation rates of other GPCR antagonists have indicated that slow receptor–ligand dissociation can result in an unusual pattern of functional antagonism known as insurmountable antagonism, in which the antagonist decreases the E_{max} of the functional response to an agonist [22,28,30,31,38,39]. By contrast, more rapidly dissociating compounds do not reduce the E_{max} (surmountable antagonism). Here we tested the functional consequence of the differences of nonpeptide antagonist dissociation rate by measuring antagonism of GnRH-stimulated inositol phosphates accumulation in RBL cells expressing the human GnRH receptor. The GnRH dose response was measured alone and in the presence of multiple concentrations of antagonist (Fig. 5) and the effect on GnRH EC_{50} and E_{max} determined (Fig. 6). GnRH robustly stimulated inositol phosphates accumulation (Fig. 5), with a $-\log EC_{50}$ of 8.48 ± 0.08 (n = 14, EC_{50} of 3.3 nM), consistent with previous studies [40]. NBI 42902 and Uracil-1 produced a dose-dependent rightward shift of the GnRH dose–response curve (Figs. 5A and B and 6A) without suppressing the E_{max} (Fig. 6B). However, Uracil-2 and Uracil-3 reduced the GnRH E_{max} in a concentration-dependent manner as well as producing a rightward shift of the dose–response curve (Figs. 5C and D and 6A and B). Therefore the two compounds that dissociated the most slowly (Uracil-2 and Uracil-3) displayed insurmountable antagonism of GnRH-stimulated inositol phosphates accumulation, whereas the two compounds that dissociated more rapidly (NBI 42902 and Uracil-1) displayed surmountable antagonism. This finding suggests that the slow dissociation rate of Uracil-2 and Uracil-3 was at least partially responsible for insurmountable antagonism of GnRH-stimulated signaling.

4. Discussion

A large diversity of nonpeptide ligands have been developed for the GnRH receptor, with the aim of developing orally available agents for the treatment of diseases associated with the reproductive-endocrine axis [9–16,41]. The SAR of these antagonists has typically been assessed using measurements of ligand affinity in radioligand displacement assays or ligand potency in functional inhibition experiments. The aim of this study was to investigate the kinetics of uracil-series nonpeptide antagonist interaction with the GnRH receptor, utilizing a novel nonpeptide radioligand, [^{3}H] NBI 42902. The principle findings are: (1) Uracil-2 and Uracil-3 dissociated very slowly from the receptor; (2) differing substitutions at the 2-position of the benzyl group (at position 1 of the uracil) markedly affected the dissociation rate constant of the ligands without appreciably affecting

the ligand association rate constant; (3) this kinetic SAR was poorly resolved by measuring the apparent affinity in standard competition binding experiments, an effect that was quantitatively consistent with a lack of receptor–ligand equilibration; (4) the differences in dissocation rate constant were correlated with differences in the functional antagonist behavior for blocking GnRH-stimulated inositol phosphate accumulation. The more rapidly dissociating antagonists did not reduce the GnRH E_{max} (surmountable antagonism), whereas the more slowly dissociating ligands strongly reduced the GnRH E_{max} (insurmountable antagonism). Taken together, evaluating the receptor binding kinetics of these nonpeptide antagonists revealed a ligand SAR, not evident in standard competition binding experiments, which was implicated in the mode of functional antagonism of GnRH-stimulated intracellular signaling.

Some of the GnRH receptor antagonists tested in this study dissociated very slowly from the receptor, for example Uracil-2 ($t_{1/2}$ for dissociation of 14 h) and Uracil-3 (>43 h). Slow receptor–ligand dissociation might offer potential therapeutic benefits compared with a more rapidly dissociating ligand. Slowly dissociating antagonists of the AT_1 receptor such as candesartan produce prolonged blockade of angiotensin-mediated blood-vessel contraction [26], compared with more rapidly dissociating compounds such as losartan. This prolonged duration of action has been observed clinically (reviewed in Ref. [33]). For example, in a comparative study, the antihypertensive effect of candesartan persisted 24 h after dosing whereas blood pressure returned to baseline 24 h after administration of losartan [32]. Slowly dissociating AT_1 receptor antagonists may also provide greater maximal hypertensive effects compared with more rapidly dissociating ligands. Meta analysis of clinical data [42] and direct comparison studies [32,43] suggest candesartan produces a greater hypertensive effect than losartan, that cannot be achieved by increasing exposure of the more rapidly-dissociating losartan [42,44]. By analogy, it is conceivable that slowly dissociating antagonists of the GnRH receptor might produce prolonged and/or greater suppression of pituitary gonadotropins.

Insurmountable antagonism of GnRH-stimulated inositol phosphates accumulation was observed with the most slowly dissociating nonpeptide antagonists (Uracil-2 and Uracil-3), whereas the more rapidly dissociating compounds did not affect the GnRH E_{max} (NBI 42902 and Uracil-1). This observation implies that slow dissociation from the receptor at least partially contributes to the insurmountable behavior of the antagonist, as observed previously for a variety of GPCRs [22,28,30,31,38,39]. For the GnRH receptor the molecular basis of slow dissociation and its mechanistic relationship with insurmountability require further investigation. The structure–activity relationship of the dissociation rate constant indicates that a $-CF_3$ group is favored at position R1 (Fig. 1) over the other substituents (Table 1). One possible explanation for this structure–activity relationship is that slow dissociation results from the greater electron withdrawing capacity of the $-CF_3$ group on the phenyl ring, which may stabilize interactions with aromatic amino acids of the receptor [34]. It is also not presently known whether a receptor conformational change is involved in slow antagonist dissociation and insurmountable antagonism, as has been proposed for candasartan interaction with the AT_1 receptor [25,45,46].

The potentially important differences of receptor interaction identified kinetically were not evident in standard competition binding experiments. The differentiation of the dissociation rate constant was >50-fold between Uracil-1 and Uracil-3, whereas the apparent K_i from competition binding experiments varied only 8.2-fold. Notably, the apparent K_i of the insurmountable antagonist Uracil-3 (44 pM) was not significantly different from that of the surmountable antagonist NBI 42902 (90 pM), whereas the former compound dissociated at least 10-fold more slowly than the latter. These findings indicate the potential importance of measuring ligand–receptor binding kinetics in fully resolving SAR for GnRH receptor nonpeptide antagonists. Similarly, considering receptor binding kinetics has been important in defining ligand SAR for other GPCRs such as muscarinic receptors [21], the μ opioid receptor [22] and the α_2-adrenergic receptor [47]. This phenomenon is also well-described in the early studies of Aranyi and coworkers on steroid receptors [20,48,49]. These studies have indicated that erroneous estimates of K_i can result in competition assays owing to lack of equilibration resulting from a slow rate-limiting receptor interaction [18,20]. In this study we demonstrated by simulation with Eq. (3) that the apparent K_i values obtained in competition experiments were predicted by the association and dissociation rate constants of the ligands. This finding is consistent with lack of equilibration underlying the erroneous estimates of nonpeptide antagonist affinity in the standard competition assay. Overall these results suggest that kinetics should be considered in evaluating the SAR of high-affinity GnRH receptor antagonists.

In summary, we have evaluated the kinetics of nonpeptide antagonist ligand interaction with the GnRH receptor utilizing a novel radioligand, [^{3}H] NBI 42902, and found a structure–activity relationship defined by the dissociation rate of the ligand from the receptor. This difference of receptor ligand interaction was poorly resolved in standard competition binding experiments but appears to correlate with the mode of functional antagonism (insurmountable versus surmountable). Given the potential importance of slow ligand dissociation and insurmountability in the therapeutic effect of other GPCR antagonists, these findings could be useful in the further development of nonpeptide antagonists targeting the GnRH receptor.

Acknowledgement

Michael Brown is gratefully acknowledged for excellent technical contributions.

REFERENCES

[1] Cheng KW, Leung PC. The expression, regulation and signal transduction pathways of the mammalian gonadotropin-releasing hormone receptor. Can J Physiol Pharmacol 2000;78(12):1029–52.
[2] Millar RP, Lu ZL, Pawson AJ, Flanagan CA, Morgan K, Maudsley SR. Gonadotropin-releasing hormone receptors. Endocr Rev 2004;25(2):235–75.

[3] Naor Z. Signal transduction mechanisms of Ca2+ mobilizing hormones: the case of gonadotropin-releasing hormone. Endocr Rev 1990;11(2):326–53.
[4] Huirne JA, Lambalk CB. Gonadotropin-releasing-hormone-receptor antagonists. Lancet 2001;358(9295):1793–803.
[5] Conn PM, Crowley Jr WF. Gonadotropin-releasing hormone and its analogs. Annu Rev Med 1994;45:391–405.
[6] Tomera K, Gleason D, Gittelman M, Moseley W, Zinner N, Murdoch M, et al. The gonadotropin-releasing hormone antagonist abarelix depot versus luteinizing hormone releasing hormone agonists leuprolide or goserelin: initial results of endocrinological and biochemical efficacies in patients with prostate cancer. J Urol 2001;165(5):1585–9.
[7] Garnick MB, Campion M. Abarelix Depot, a GnRH antagonist, v LHRH superagonists in prostate cancer: differential effects on follicle-stimulating hormone. Abarelix Depot study group. Mol Urol 2000;4(3):275–7.
[8] Halmos G, Schally AV, Pinski J, Vadillo-Buenfil M, Groot K. Down-regulation of pituitary receptors for luteinizing hormone-releasing hormone (LH-RH) in rats by LH-RH antagonist Cetrorelix. Proc Natl Acad Sci USA 1996;93(6):2398–402.
[9] Zhu YF, Chen C, Struthers RS. Nonpeptide gonadotropin releasing hormone antagonists. Ann Rep Med Chem 2004;39:99–110.
[10] Armer RE, Smelt KH. Non-peptidic GnRH receptor antagonists. Curr Med Chem 2004;11(22):3017–28.
[11] DeVita RJ, Walsh TF, Young JR, Jiang J, Ujjainwalla F, Toupence RB, et al. A potent, nonpeptidyl 1H-quinolone antagonist for the gonadotropin-releasing hormone receptor. J Med Chem 2001;44(6):917–22.
[12] Tucci FC, Zhu YF, Struthers RS, Guo Z, Gross TD, Rowbottom MW, et al. 3-[(2R)-Amino-2-phenylethyl]-1-(2,6-difluorobenzyl)-5-(2-fluoro-3-methoxyp henyl)- 6-methylpyrimidin-2,4-dione (NBI 42902) as a potent and orally active antagonist of the human gonadotropin-releasing hormone receptor. Design, synthesis, and in vitro and in vivo characterization. J Med Chem 2005;48(4):1169–78.
[13] Reinhart GJ, Xie Q, Liu XJ, Zhu YF, Fan J, Chen C, et al. Species selectivity of nonpeptide antagonists of the gonadotropin-releasing hormone receptor is determined by residues in extracellular loops II and III and the amino terminus. J Biol Chem 2004;279(33):34115–22.
[14] Sasaki S, Cho N, Nara Y, Harada M, Endo S, Suzuki N, et al. Discovery of a thieno[2,3-d]pyrimidine-2,4-dione bearing a *p*-methoxyureidophenyl moiety at the 6-position: a highly potent and orally bioavailable non-peptide antagonist for the human luteinizing hormone-releasing hormone receptor. J Med Chem 2003;46(1):113–24.
[15] Cui J, Smith RG, Mount GR, Lo JL, Yu J, Walsh TF, et al. Identification of Phe313 of the gonadotropin-releasing hormone (GnRH) receptor as a site critical for the binding of nonpeptide GnRH antagonists. Mol Endocrinol 2000;14(5):671–81.
[16] Struthers RS, Xie, et al., Pharmacologic characterization of NBI 42902, a novel non-peptide antagonist of the human GnRH receptor. Submitted for publication.
[17] Paton WDM. A kinetic approach to the mechanism of drug action. Adv Drug Res 1966;3:57–80.
[18] Motulsky HJ, Mahan LC. The kinetics of competitive radioligand binding predicted by the law of mass action. Mol Pharmacol 1984;25(1):1–9.
[19] Burgen ASV. The drug-receptor complex. J Pharm Pharmacol 1966;18:137–49.
[20] Aranyi P. Kinetics of the hormone–receptor interaction. Competition experiments with slowly equilibrating ligands. Biochim Biophys Acta 1980;628(2):220–7.
[21] Waelbroeck M, Camus J, Christophe J. Determination of the association and dissociation rate constants of muscarinic antagonists on rat pancreas: rank order of potency varies with time. Mol Pharmacol 1989;36(3):405–11.
[22] Cassel JA, Daubert JD, DeHaven RN. [(3)H]Alvimopan binding to the micro opioid receptor: comparative binding kinetics of opioid antagonists. Eur J Pharmacol 2005;520(1–3):29–36.
[23] Severne Y, Ijzerman A, Nerme V, Timmerman H, Vauquelin G. Shallow agonist competition binding curves for beta-adrenergic receptors: the role of tight agonist binding. Mol Pharmacol 1987;31(1):69–73.
[24] Vauquelin G, Van Liefde I, Vanderheyden P. Models and methods for studying insurmountable antagonism. Trends Pharmacol Sci 2002;23(11):514–8.
[25] Lew MJ, Ziogas J, Christopoulos A. Dynamic mechanisms of non-classical antagonism by competitive AT(1) receptor antagonists. Trends Pharmacol Sci 2000;21(10):376–81.
[26] Morsing P, Adler G, Brandt-Eliasson U, Karp L, Ohlson K, Renberg L, et al. Mechanistic differences of various AT1-receptor blockers in isolated vessels of different origin. Hypertension 1999;33(6):1406–13.
[27] Fierens FL, Vanderheyden PM, De Backer JP, Vauquelin G. Insurmountable angiotensin AT1 receptor antagonists: the role of tight antagonist binding. Eur J Pharmacol 1999;372(2):199–206.
[28] Fierens F, Vanderheyden PM, De Backer JP, Vauquelin G. Binding of the antagonist [3H]candesartan to angiotensin II AT1 receptor-transfected Chinese hamster ovary cells. Eur J Pharmacol 1999;367(2–3):413–22.
[29] Mathiesen JM, Christopoulos A, Ulven T, Royer JF, Campillo M, Heinemann A, et al. On the mechanism of interaction of potent surmountable and insurmountable antagonists with the prostaglandin D2 receptor CRTH2. Mol Pharmacol 2006;69(4):1441–53.
[30] Burris KD, Sanders-Bush E. Unsurmountable antagonism of brain 5-hydroxytryptamine2 receptors by (+)-lysergic acid diethylamide and bromo-lysergic acid diethylamide. Mol Pharmacol 1992;42(5):826–30.
[31] Anthes JC, Gilchrest H, Richard C, Eckel S, Hesk D, West Jr RE, et al. Biochemical characterization of desloratadine, a potent antagonist of the human histamine H(1) receptor. Eur J Pharmacol 2002;449(3):229–37.
[32] Lacourciere Y, Asmar R. A comparison of the efficacy and duration of action of candesartan cilexetil and losartan as assessed by clinic and ambulatory blood pressure after a missed dose, in truly hypertensive patients: a placebo-controlled, forced titration study. Am J Hypertens 1999;12(12 Pt 1–2):1181–7.
[33] Gradman AH. AT(1)-receptor blockers: differences that matter. J Hum Hypertens 2002;16(Suppl 3):S9–16.
[34] Betz SF, Reinhart GJ, Lio FM, Chen C, Struthers RS. Overlapping, nonidentical binding sites of different classes of nonpeptide antagonists for the human gonadotropin-releasing hormone receptor. J Med Chem 2006;49(2):637–47.
[35] Benjamin ER, Haftl SL, Xanthos DN, Crumley G, Hachicha M, Valenzano KJ. A miniaturized column chromatography method for measuring receptor-mediated inositol phosphate accumulation. J Biomol Screen 2004;9(4):343–53.
[36] Hoare SR, Sullivan SK, Ling N, Crowe PD, Grigoriadis DE. Mechanism of corticotropin-releasing factor type I receptor regulation by nonpeptide antagonists. Mol Pharmacol 2003;63(3):751–65.
[37] Cheng Y, Prusoff WH. Relationship between the inhibition constant (K1) and the concentration of inhibitor which causes 50 per cent inhibition (I_{50}) of an enzymatic reaction. Biochem Pharmacol 1973;22(23):3099–108.
[38] Olins GM, Chen ST, McMahon EG, Palomo MA, Reitz DB. Elucidation of the insurmountable nature of an angiotensin

receptor antagonist, SC-54629. Mol Pharmacol 1995;47(1):115–20.
[39] Gillard M, Van Der Perren C, Moguilevsky N, Massingham R, Chatelain P. Binding characteristics of cetirizine and levocetirizine to human H(1) histamine receptors: contribution of Lys(191) and Thr(194). Mol Pharmacol 2002;61(2):391–9.
[40] McArdle CA, Forrest-Owen W, Willars G, Davidson J, Poch A, Kratzmeier M. Desensitization of gonadotropin-releasing hormone action in the gonadotrope-derived alpha T3-1 cell line. Endocrinology 1995;136(11):4864–71.
[41] Tucci FC, Zhu YF, Guo Z, Gross TD, Connors Jr PJ, Struthers RS, et al. A novel synthesis of 7-aryl-8-fluoro-pyrrolo[1,2-a]pyrimid-4-ones as potent, stable GnRH receptor antagonists. Bioorg Med Chem Lett 2002;12(23):3491–5.
[42] Hansson L. The relationship between dose and antihypertensive effect for different AT1-receptor blockers. Blood Press Suppl 2001;(3):33–9.
[43] Bakris G, Gradman A, Reif M, Wofford M, Munger M, Harris S, et al. Antihypertensive efficacy of candesartan in comparison to losartan: the CLAIM study. J Clin Hypertens (Greenwich) 2001;3(1):16–21.
[44] Gradman AH, Arcuri KE, Goldberg AI, Ikeda LS, Nelson EB, Snavely DB, et al. A randomized, placebo-controlled, double-blind, parallel study of various doses of losartan potassium compared with enalapril maleate in patients with essential hypertension. Hypertension 1995;25(6):1345–50.
[45] Vauquelin G, Morsing P, Fierens FL, De Backer JP, Vanderheyden PM. A two-state receptor model for the interaction between angiotensin II type 1 receptors and non-peptide antagonists. Biochem Pharmacol 2001;61(3):277–84.
[46] Takezako T, Gogonea C, Saad Y, Noda K, Karnik SS. ''Network leaning'' as a mechanism of insurmountable antagonism of the angiotensin II type 1 receptor by non-peptide antagonists. J Biol Chem 2004;279(15):15248–57.
[47] Convents A, De Backer JP, Convents D, Vauquelin G. Tight agonist binding may prevent the correct interpretation of agonist competition binding curves for alpha 2-adrenergic receptors. Mol Pharmacol 1987;32(1):65–72.
[48] Aranyi P. Kinetics of the glucocorticoid hormone-receptor interaction. False association constants determined in slowly equilibrating systems. Biochim Biophys Acta 1979;584(3):529–37.
[49] Aranyi P. Dependence of rate constants of the glucocorticoid hormone–receptor interaction on steroid structure. J Steroid Biochem 1982;17(2):137–41.